Available online at www.sciencedirect.com
ScienceDirect
Ceramics International 35 (2009) 2915–2920
CERAMICS INTERNATIONAL
www.elsevier.com/locate/ceramint

Influence of processing atmosphere on the microstructural evolution of submicron alumina powder during sintering

A.S.A. Chinelatto [a,*], R. Tomasi [b]

[a] Department of Materials Engineering, State University of Ponta Grossa, Av. Gal. Carlos Cavalcanti, 4748, Ponta Grossa 84030-900, PR, Brazil
[b] Department of Materials Engineering, Federal University of São Carlos, 13565-905 São Carlos, SP, Brazil

Received 12 December 2008; received in revised form 28 January 2009; accepted 30 March 2009
Available online 24 April 2009

Abstract

Investigations into the sintering of submicron oxide powders have revealed interesting behavior, particularly insofar as it concerns their microstructural evolution in the early, low temperature transformations during heating. In this work, experiments were conducted on a submicron alumina powder, whose microstructural evolution and densification were characterized after sintering from 900 °C to 1400 °C in air, dry air and high vacuum (10^{-8} atm). The results indicated that the processing atmosphere strongly influences the particle size distribution at low temperatures before shrinkage occurs. Shrinkage began concomitantly with grain growth and the sintering atmosphere influenced the sintering kinetics. This factor, which is associated with previous narrowing of the particle size distribution, may affect grain growth and densification during the final stage of sintering.

Keywords: Sintering; Alumina; Atmosphere

1. Introduction

The engineering applications of technical ceramics are generally related to microstructure-controlled properties. The main objective of processing is to produce the desired microstructure, which frequently involves obtaining high density and small grain size. In recent years, the significant improvements in properties brought about by submicron and nanostructured ceramic materials and the availability of many different production routes for ultrafine and nano-sized ceramic powders have led researchers to focus increasingly on the processing of these types of powders. The present research, too, was motivated by ultrafine powder processing problems, since defect-free and homogeneous microstructures are crucial for potential applications. Although several sintering routes are available for the production of high density and controlled grain size ceramics, such as the use of sintering additives, pressure sintering and colloidal processing of near-monosized sub-micron powders, the optimization of conventional pressureless sintering has the advantage of simplicity and economy [1–9].

In pressureless sintering, in addition to the important role of control over the powders characteristics, control of the sintering process itself is crucial for the final density and microstructure. The main control parameters are the time–temperature schedule and atmosphere. In the time–temperature schedule, the heating rate allows for different solutions: control of the heating rate to influence the microstructural evolution or to produce changes in the powder compact during heating to a maximum constant sintering temperature [2,3,5–12]. Important transformation processes that occur at low temperatures, particularly before or at the beginning of the densifying stages of sintering, have been reported for the so-called submicron, ultrafine and nano-sized ceramic powders [5–11] These processes are due to the high specific surface area (SSA) of fine powders; and the most important process is the coarsening produced by non-densifying surface diffusion or evaporation/condensation mechanisms [5–8]. In the case of nano-sized powders, another mechanism of sintering densification, called particle repacking, was identified as resulting from coarsening [10].

The influence of the processing atmosphere on the sintering behavior of alumina has been studied extensively [11–16] and

* Corresponding author. Tel.: +55 42 3220 3079; fax: +55 42 3220 3079.
E-mail address: adriana@uepg.br (A.S.A. Chinelatto).

0272-8842/$36.00
doi:10.1016/j.ceramint.2009.03.037

the sintering atmosphere was shown to significantly affect the above-mentioned low temperature processes in submicron-sized alumina powder [17,18]. This effect of the sintering atmosphere was manifested in the form of drastic variations in the final grain size, including a significantly smaller grain size after sintering under high-vacuum atmosphere.

Franks and Gan [19] made a complete review of the interaction between water and the alumina surface. Water can be incorporated into the alumina crystal structure, resulting in the formation of aluminum hydroxides, and there are several types of surface hydroxyl groups [20,21]. Some studies of Al_2O_3 have shown that the dehydroxylation occurring during high temperature treatments can produce surface defect sites on Al_2O_3, which are believed to consist of Al^{3+} sites adjacent to anionic vacancies [22]. It was observed that water vapor influences the process of nucleation and growth of α-Al_2O_3 from γ-Al_2O_3 and the accelerated kinetics is believed to be due to increased surface diffusion [23,24].

In this work, experiments were conducted on a submicron alumina powder without sintering aids, in which the microstructural evolution and densification were characterized from 900 °C to 1400 °C under air, dried air and high vacuum (10^{-8} atm). The effects on the evolution of the powder compact structure were investigated.

2. Experimental procedure

A commercial, high-purity Al_2O_3 powder (AKP53, Sumitomo Chemical America, Inc.) was ball milled to break up agglomerates. The powder was dispersed in isopropyl alcohol with 0.2 wt% of PABA (4-aminobenzoic acid) and 0.5 wt% of oleic acid and ball milled for 10 h with 5 mm zirconia balls (ball:powder mass ratio of 2:1) in a polypropylene vial. The particle size distribution of the resulting suspension was determined by sedimentation in a Micromeritics Sedigraph 5100 apparatus, for qualitative control of the deagglomeration process. The suspension was dried in air at 70 °C and the powder lightly ground in a mortar and sifted through an 80-mesh nylon sieve.

The specimens for sintering were uniaxially pressed under 80 MPa to form cylindrical compacts (10 mm in diameter and about 5 mm in height) and isostatically cold-pressed under 200 MPa. The green density of the specimens was about 57.5 ± 0.7% of theoretical density (%TD). The specimens were heat-treated for 1 h at 600 °C in air to remove the binders.

The sintering experiments were performed using a dilatometer NETZSCH-DIL 402C for experiments in air and under high vacuum (~10^{-8} atm). The samples were sintered for 1 h in air and high vacuum at temperatures of 900, 1000, 1100, 1200, 1250, 1300 and 1400 °C, applying a heating rate of 15 °C/min. Considering the results of these experiments, a second set of experiments was performed with dry air (synthetic air) in order to evaluate the role of water vapor in ambient air.

The density of the sintered samples was measured by the Archimedes method in deionized water. Microstructural analyses were performed by high resolution SEM (Philips-XL30-FEG) of the fracture surface of low-density sintered samples and of the polished and thermally etched surfaces of high density sintered samples. The grain size distribution was measured based on an appropriate number of SEM images of each sample. A large number of micrographs were obtained from each sample, allowing for the measurement of more than 150 individual grains. The grain size distributions were represented as Gaussian fits to the data histograms. Additionally, the specific surface area (SSA) of low-density samples was measured by the BET method (Micromeritics-Gemini 2370).

3. Results and discussion

Fig. 1 shows the relative density of samples after sintering in air and in vacuum furnaces for 1 h at different temperatures. The most significant effect was the shift to lower temperatures in the curve obtained under vacuum. This shift was approximately 100° and was practically constant, i.e., it remained about 100° from the shrinkage startup temperature up to the final stage of sintering (about 95% of TD).

The final density was found to increase due to the vacuum; however, as will be discussed later, the residual porosity in samples vacuum sintered at 1400 °C was mostly due to large pores introduced during the forming process. It is worth noting that the atmosphere altered the temperature at which densification began, suggesting that a difference in the powder compact due to the atmosphere was established at low temperatures.

The differences in the sintering atmosphere (vacuum or air) were also evident at low temperatures through the variation in the SSA of the powder compact as a function of sintering temperature, as shown in Fig. 2. Before sintering, the powder's SSA was 19.5 m^2/g. The greatest difference in the SSA of the sintered samples was observed with a heat treatment of 900 °C, the lowest sintering temperature used in this study. Heating under air resulted in a more marked decrease in SSA than under vacuum. The difference in SSA between the two samples decrease as the sintering temperature increased. The SSA of the

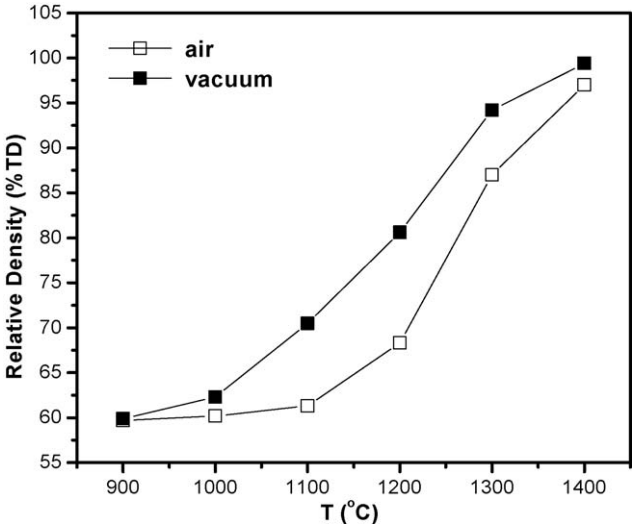

Fig. 1. Relative density (percentage of theoretical density) vs. sintering temperature of samples sintered in air and in vacuum.

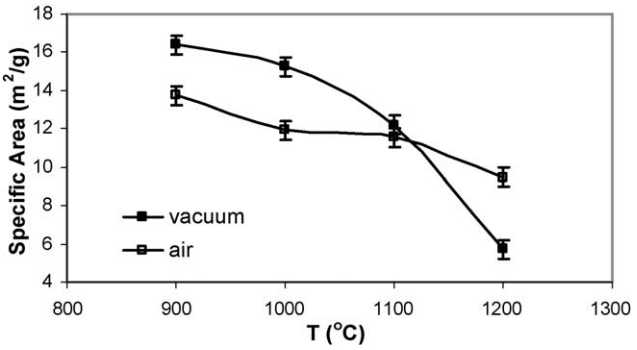

Fig. 2. SSA vs. sintering temperature of samples sintered in vacuum and in air.

two samples was almost equal at 1100 °C. The decrease in SSA under vacuum at 1100 °C and 1200 °C resulted from the densification process, which, as shown in Fig. 1, occurred in a range of lower temperatures than in air sintering. These results suggest that an air atmosphere produces a significant decrease of SSA during heating, hastening the coarsening process in the low temperature pre-densification stages of sintering and thus affecting subsequent densification at higher sintering temperatures. The coarsening process was analyzed by direct observation of the particles or grain size in the sintered samples.

Figs. 3–5 show SEM micrographs of the fracture surface of samples sintered at different temperatures in air and in vacuum. The sample sintered in high vacuum at 1000 °C (Fig. 3(b)) shows the presence of very fine particles on the surface of the larger ones. In high vacuum at 1100 °C (Fig. 4(b)), such fine particles are still visible and they are partially coalesced with the large particles around them. After sintering in air at 1000 °C (Fig. 3(a)), the very fine particles are absent and the morphology reveals the coalescence of the remaining small particles with the larger particles and the growth of necks between particles. In air at 1100 °C (Fig. 4(a)), the grains are spherical and also display some neck formation. On the other hand, at 1200 °C (Fig. 5), the sample sintered in vacuum presents a more advanced sintering process with faceted grains of intergranular fracture, which is consistent with the previous observation that, in vacuum, the densification process begins at a lower temperature.

Fig. 6 depicts the results of these samples' grain size distribution in terms of the Gaussian fit of the normalized frequency count of measured grain size. This simplified representation of the grain size distribution emphasizes two important observations: the most effective coarsening process resulting from the air atmosphere is revealed by the increase in mean particle size. At temperatures of up to 1200 °C in vacuum, the increase in grain size is negligible and the grain size distribution in this lower range of temperatures is narrowed slightly by the decreasing numbers of the finest particles. In both cases, when the mean size begins to increase in the 900 °C to 1000 °C range in air or at 1200 °C in vacuum, grain growth is accompanied by a broadening of grain size distribution.

Fig. 7 presents the mean grain size versus relative density plot for samples sintered in air and in vacuum. The curves show that grain growth under vacuum sintering began at a higher

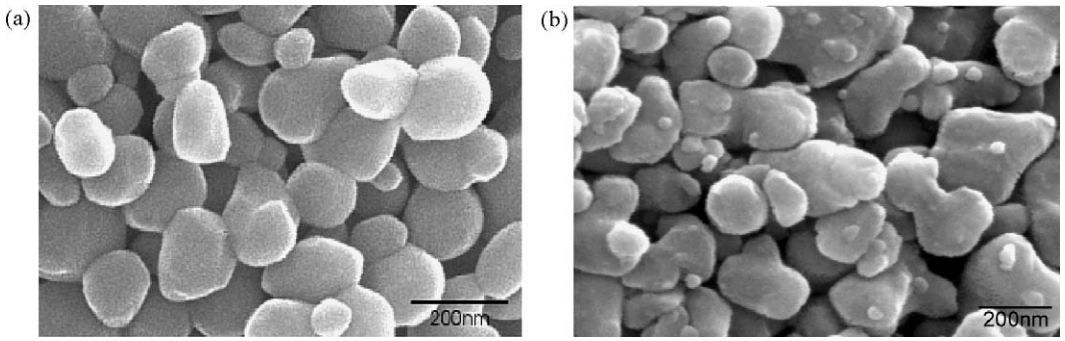

Fig. 3. SEM micrographs of the fracture surface of samples obtained from the as received commercial Al_2O_3 powder, sintered for 1 h at 1000 °C: (a) in air, and (b) in high vacuum.

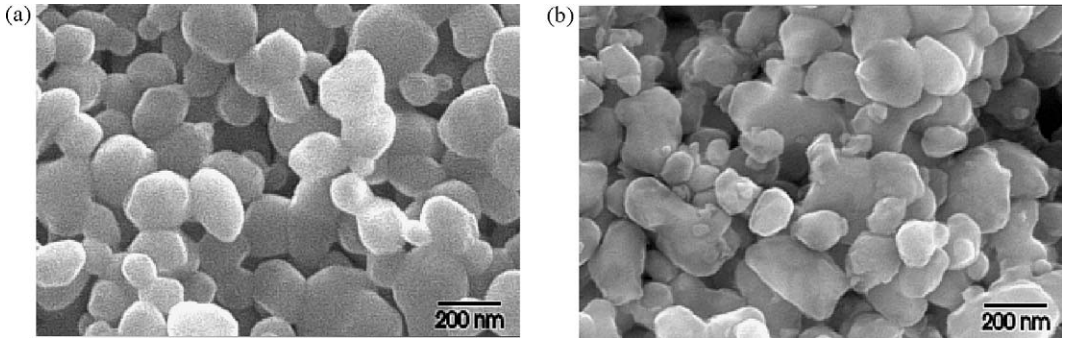

Fig. 4. SEM micrographs of the fracture surface of samples obtained from the as received commercial Al_2O_3 powder, sintered for 1 h at 1100 °C: (a) in air, and (b) in high vacuum.

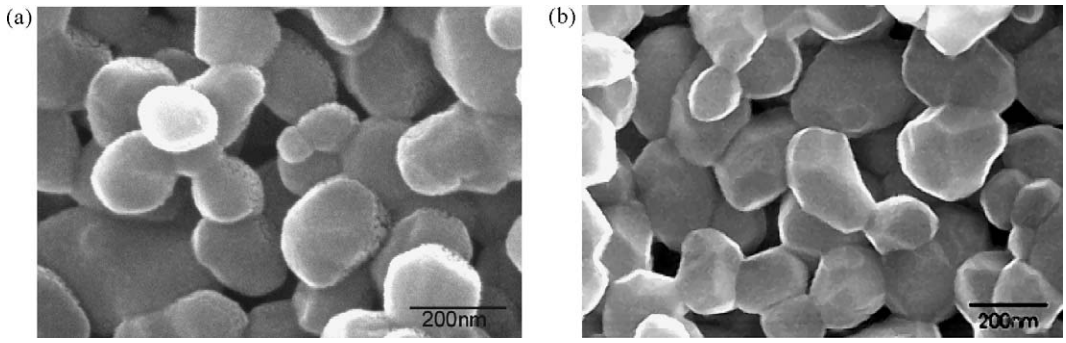

Fig. 5. SEM micrographs of the fracture surface of samples obtained from the as received commercial Al_2O_3 powder, sintered for 1 h at 1200 °C: (a) in air, and (b) in high vacuum.

density than in air so that, at approximately 96%TD, which was reached at 1300 °C, the grain size was about 400 nm. In air, the same grain size was reached at about 85%TD, while the grain size was approximately 600 nm when a density of around 96%TD was reached. This degree of densification in air (96%TD), see Fig. 1, was attained only at 1400 °C. In the vacuum sintered samples, the increase of sintering temperature to 1400 °C led to a pronounced grain growth, with density increasing from 95%TD to about 98.5%TD, which was attributed to the absence of pores at the grain boundaries. The microstructure contained a few large pores dispersed in a completely dense microstructure. Therefore, the final density was probably the maximum possible density that can be achieved when sintering at 1400 °C, so that the remaining sintering time is characterized mainly by grain growth. Possibly, the final density (about 98.5%TD) is reached in an intermediate condition of vacuum sintering, by sintering at a temperature below 1400 °C or for a shorter sintering time at 1400 °C, so that the final density is attained with less grain growth. The presence of large pores was probably due to interagglomerated pores not eliminated by the pressing process.

One known effect of the processing atmosphere on the surface of alumina at low temperatures is caused by the presence of water vapor [16,17]. This effect was verified by repeating the above experiments in synthetic dry air. Fig. 8 shows the SSA versus sintering temperature curve obtained in dry air with a 15 °C/min heating rate compared with the SSA resulting from sintering in air and in vacuum (same results as in Fig. 2). In dry air, the variation in the SSA during sintering

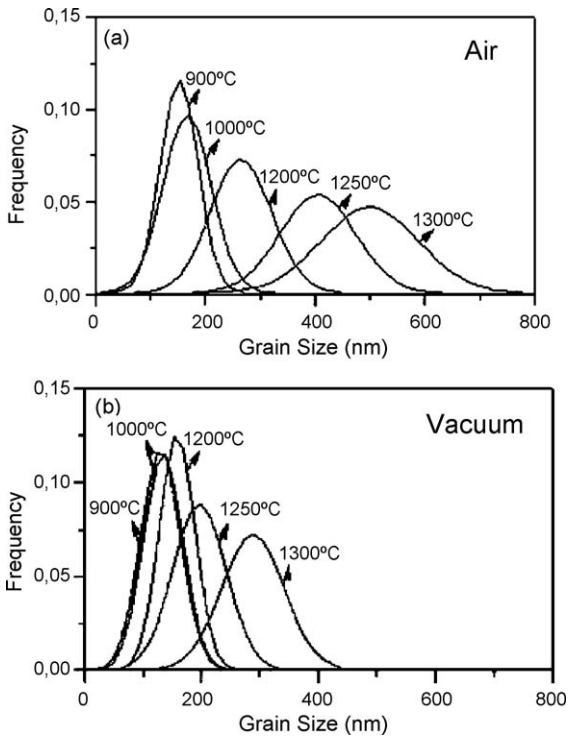

Fig. 6. Grain size distribution of samples obtained from the as received commercial Al_2O_3 powder, sintered for 1 h at different temperatures: (a) in air, and (b) in high vacuum.

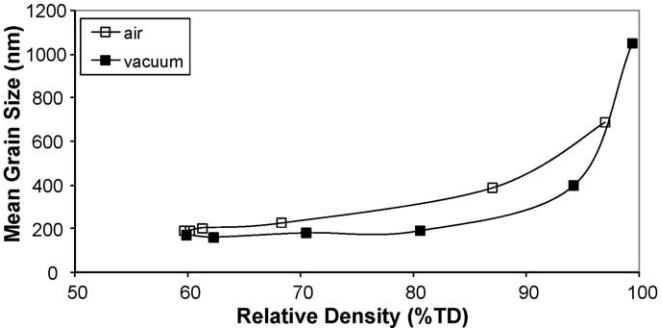

Fig. 7. Mean grain size vs. relative density of samples sintered for 1 h in vacuum and in air.

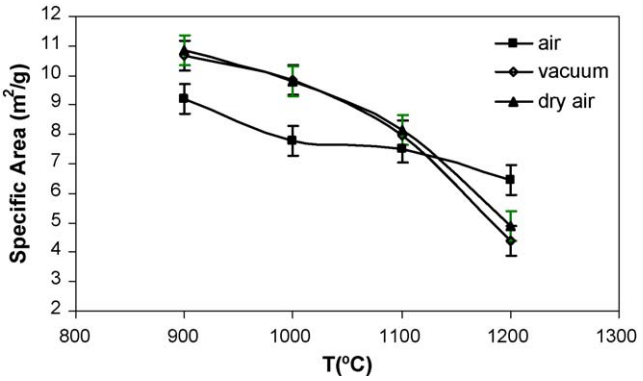

Fig. 8. SSA vs. sintering temperature, at a heating rate of 15 °C/min, in vacuum, in air, and in dry air.

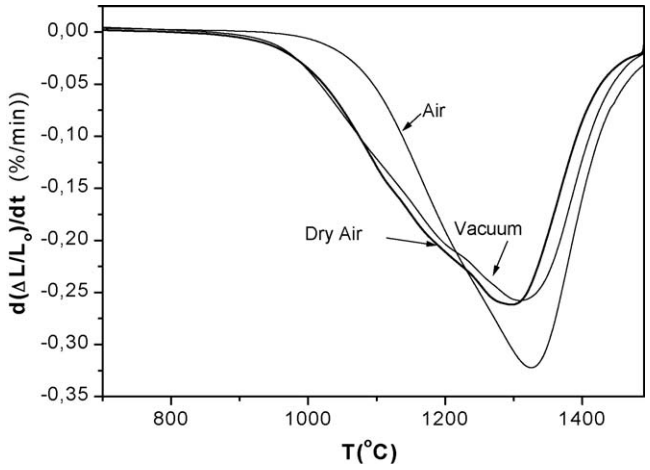

Fig. 9. Linear shrinkage rate vs. temperature during heating in dilatometer, at a constant heating rate of 15 °C/min in air, in dry air, and in high vacuum.

showed the same behavior as in vacuum. The shrinkage results from the dilatometer showed that the same behavior occurred in dry air and in high vacuum, particularly at the beginning of densification (see Fig. 9).

The results of the linear shrinkage rate shown in Fig. 9 also reveal that the sintering behavior in air differs from that in dry air and vacuum only insofar as the densification startup temperature, as shown in Fig. 1, and the sintering rate are concerned. These results, which agree with observations of the SSA and grain size distribution, suggest that the most important effect of the atmosphere occurs during heating in the low temperature pre-densification stages of sintering and are due to the presence of water vapor. The higher partial water vapor pressure in ambient air produces a significant decrease of SSA and faster coarsening. In ambient air, the non-densifying coarsening process is associated with increased mean grain size and broadening of the grain size distribution, while, under vacuum and probably under low water vapor pressure, the grain size distribution is narrowed by the elimination of some of the finest particles, leading to a small amount of coarsening. This difference in grain size and in grain size distribution due to water vapor is a determining factor of the behavior of densification and grain size evolution during the subsequent stages of sintering.

During the sintering process, compact powders can reduce free energy by densification and by grain growth (or coarsening). These processes not only occur concurrently but also interact, so that the rate of one depends on the extent of the other. The possible mechanisms that can cause particle coarsening are surface diffusion or gaseous phase transport, while densification occurs by volumetric diffusion and by grain boundary diffusion [1].

It is reported in the literature that, at low temperatures, alumina undergoes neck growth or decrease of surface area without undergoing densification. Hence, evaporation–condensation processes or surface diffusion can be dominant mechanisms for atomic transport. However, Ready and Kuczniski [24] demonstrated that, for alumina, the evaporation–condensation mechanism is important only for very low partial pressures of oxygen, in the order of $\sim 10^{-19}$ atm at 900 °C and $\sim 10^{-16}$ atm at 1100 °C. Thus, vapor transport in alumina can be disregarded, and surface diffusion can be considered the predominant mechanism at low temperatures. At higher temperatures, alumina densifies through volumetric diffusion and grain boundary diffusion [25]. When surface diffusion is rapid enough to affect particle coarsening at low temperatures, the densification rate decreases due to the reduction of the surface area, which is the driving force for the densification process [26].

In this work, sintering in air led to greater particle coarsening at low temperatures and a lower densification rate than sintering under high vacuum and dry air. This effect can be attributed to the greater surface diffusion that occurs during sintering in air.

According to Bagwell and Messing [23], the mechanisms that can contribute to increased diffusion by water vapor are gaseous phase transport, changes in surface energies and increased concentration of defects.

As mentioned earlier, the mechanism of vapor transport in alumina can be disregarded due to the low vapor pressure of species containing aluminum ($<10^{-15}$ atm). The change in surface energy due to water vapor adsorption is another mechanism that can be considered to explain the effect of water vapor on particle coarsening. In a study of the chemical and physical adsorption of water on the surface of α-alumina, De Leeuw and Parker [27] found that water adsorption reduces the surface energy of alumina, rendering it stable. If that effect actually predominated, the adsorbed water would diminish the coarsening effect, since the driving force for coarsening is the reduction of free energy at the surface.

The other potential mechanism for increased diffusion is the change in defect concentration due to water molecules adsorbed on the surface. Many studies [19–22,28] have shown that transition alumina and α-alumina crystals adsorb high concentrations of water molecules, which form hydroxyl in a variety of configurations and are highly mobile. The formation of hydroxyls $(OH)^{-1}$ in alumina results in local positive charges that have to be compensated by the negatively charged defects. Aluminum vacancies could be created to balance the additional charge, which would increase the aluminum diffusion coefficient. Hence, the change in defect concentration due to the adsorption of water molecules offers a reasonable explanation for the increase in surface diffusion.

4. Conclusions

Experiments were conducted to analyze the microstructural evolution of submicron alumina powder during sintering. The results revealed the strong influence of the processing atmosphere on particle size distribution at low temperatures and before shrinkage. The strong effect caused by higher coarsening rates and broader grain size distribution during sintering under ambient air atmosphere in comparison to high vacuum or dry air was attributed to the presence of water vapor. Coarsening under high vacuum or dry air atmosphere resulted in a narrow particle size distribution prior to the beginning of densification; the mean particle size did not increase and neck

growth was insignificant. These processes affected the subsequent sintering stages by shifting the sintering curve to lower temperatures and decreasing grain growth.

References

[1] R.M. German Sintering, Theory and Practice, John Wiley & Sons, New York, 1996.

[2] N.J. Shawn, Densification and coarsening during solid state sintering of ceramics: a review of the models. 1. Densification, Powder Metall. Int. 21 (1989) 16–21.

[3] M.J. Mayo, Processing of nanocrystalline ceramics from ultrafine particles, Int. Mater. Rev. 41 (1996) 85–115.

[4] L.C. Lim, P.M. Wong, M.A. Jan, Jan Microstructural evolution during sintering of near-monosized agglomerate-free submicron alumina powder compacts, Acta Mater. 48 (2000) 2263–2275.

[5] C. May-Ying, M.N. Rahaman, L.C. De Jonghe, R.J. Brook, Effect of heating rate on sintering and coarsening, J. Am. Ceram. Soc. 74 (1991) 1217–1225.

[6] M.Y. Chu, L.C. De Jonghe, M.K.F. Lin, F.J.T. Lin, Precoarsening to improve microstructure and sintering of powder compacts, J. Am. Ceram. Soc. 71 (1991) 2902–2911.

[7] F.J.T. Lin, L.C. De Jonghe, Microstructure refinement of sintered alumina by a two-step technique, J. Am. Ceram. Soc. 80 (1997) 2269–2277.

[8] F.J.T. Lin, L.C. De Jonghe, Initial coarsening and microstructural evolution of fast-fired and MgO-doped Al_2O_3, J. Am. Ceram. Soc. 80 (1997) 2891–2896.

[9] P.L. Chen, I.W. Chen, Sintering of fine oxide powders. I. Microstructural evolution, J. Am. Ceram. Soc. 79 (1996) 3129–3141.

[10] P.L. Chen, I.W. Chen, Sintering of fine oxide powders. II. Sintering mechanism, J. Am. Ceram. Soc. 80 (3) (1997) 637–645.

[11] A.M. Thompson, M.P. Harmer, Influence of atmosphere on the final-stage sintering kinetics of ultra-high-purity alumina, J. Am. Ceram. Soc. 76 (1993) 2248–2256.

[12] G.C. Wei, W.H. Rhodes, Sintering of translucid alumina in nitrogen–hydrogen gas atmosphere, J. Am. Ceram. Soc. 83 (7) (2000) 1641–1648.

[13] A.M. Thompson, M.P. Harmer, Deterioration of a classical final-stage microstructure: a study in alumina, J. Am. Ceram. Soc. 75 (4) (1992) 976–980.

[14] Y.K. Paek, K.Y. Eun, S.J.L. Kang, Effect of sintering atmosphere on densification of MgO-doped Al_2O_3, J. Am. Ceram. Soc. 71 (8) (1988) C380–C382.

[15] R.L. Coble, Sintering alumina: effect of atmosphere, J. Am. Ceram. Soc. 45 (3) (1962) 123–127.

[16] P. Miranzo, L. Taberneto, J.S. Moya, J.R. Jurado, Effect of sintering atmosphere on the densification and electrical properties of alumina, J. Am. Ceram. Soc. 73 (7) (1990) 2119–2121.

[17] E.M.A. Pallone, R. Tomasi, Sintering of alumina under high-vacuum: effect on microstructure, Cerâmica 42 (1996) 275–280 (in Portuguese).

[18] A.S.A. Chinelatto, E.M.J. Pallone, R. Tomasi, L. Del Prette, Microstructural evolution during first stage sintering of alumina, in: Proceedings of the 42nd Brazilian Ceramic Conference, Poços de Caldas, MG, Brazil, 3–6 July, 1998 (in Portuguese).

[19] G.V. Franks, Y. Gan, Charging behavior at the alumina–water interface and implications for ceramic processing, J. Am. Ceram. Soc. 90 (11) (2007) 3373–3388.

[20] T. Shirai, C. Ishizaki, K. Ishizaki, Effects of manufacturing on hydration ability of high purity α-Al_2O_3 powders, J. Ceram. Soc. Jpn. 114 (3) (2006) 286–289.

[21] T. Shirai, J.W. Li, K. Matsumaru, C. Ishizaki, K. Ishizaki, Surface hydration states of commercial high purity α-Al_2O_3 powders evaluated by temperature programmed desorption mass spectrometry and diffuse reflectance infrared Fourier transform spectroscopy, Sci. Tech. Adv. Mater. 6 (2005) 123–128.

[22] T.H. Ballinger, T. Yates Jr., IR Spectroscopic detection of Lewis acid sites on Al_2O_3 using adsorbed CO. Correlation with Al–OH group removal, Langmuir 7 (1991) 3041–3045.

[23] R.B. Bagwell, G.L. Messing, Effect of seeding and water vapor on nucleation and growth of α-Al_2O_3 from γ-Al_2O_3, J. Am. Ceram. Soc. 82 (1999) 825–832.

[24] D.W. Ready, G.C. Kuczynski, Sublimation of aluminum oxide in hydrogen, J. Am. Ceram. Soc. 49 (1) (1966) 26–29.

[25] D.W. Ready, J. Lee, T. Quadir, Vapor transport and sintering of ceramic presented at the 6th International Conference on Sintering and Related Phenomena, Notre Dame, Indiana, June, 1983.

[26] S.C. Liao, Y.J. Chen, B.H. Kear, W.E. Mayo, High pressure/low temperature sintering of nanocrystalline alumina, Nano Mater. 10 (6) (1998) 1063–1079.

[27] N.H. De Leeuw, S.C. Parker, Effect of chemisorption and physisorption of water on the surface structure and stability of α-alumina, J. Am. Ceram. Soc. 82 (11) (1999) 3209–3216.

[28] J.B. Peri, A model for the surface of γ-alumina, J. Phys. Chem. 69 (1) (1965) 220–230.